Chapter 1 Introduction and Literature Survey

1.1 Introduction

The discovery of atomically thin graphene from graphite in 2004 by Novoselov *et al.* has boosted the research in the field of two dimensional (2D) materials to find their fundamental properties and potential applications [1, 2]. The 2D materials are inherently flexible, strong, and extremely thin [3-6]. In general, the 2D material refers to a group that is weakly bonded between the layers by weak van der Waal forces. The 2D materials show variety of electronic properties such as indirect and direct band gap in the ultraviolet, visible to infrared regions and can be metals, semimetals, insulators and semiconductors [7-10]. The composition of atoms and the thickness of the layer play a crucial role to determine the fundamental properties. The confinement effect in 2D graphene and single layer of transition metal dichalcogenides (TMDs) leads to virtuous condensed-matter phenomena that are absent in their bulk counterpart. Among TMDs family, the 2D Molybdenum disulfide (MoS_2) has drawn notable attention to the scientific community in the past years due to its layer dependent electronic properties, high absorption coefficient, optical transparency and good mobility at room temperature [11-13]. A transition from indirect bandgap of ~1.3 eV in the bulk to a direct bandgap of ~1.8 eV in the monolayer is observed in MoS_2 [6]. The MoS_2 is stable in natural environment and shows excellent light absorption and thickness dependent physical behaviour suitable for optoelectronic and photonic applications [14-20]. The MoS_2 shows high quality of interface with other semiconducting materials such as Si, that helps to make heterojunction device. In this chapter we discuss fundamentals related to MoS_2 nanostructures, synthesis process and its possible applications.

1.2 Overview of 2D TMDs

The family of 2D materials encircle a wide selection of compositions including almost all the elements of the periodic table [21]. TMDs group is the largest group of 2D materials, which attracts the scientific community because of their semiconducting properties and tunable wide range bandgap.

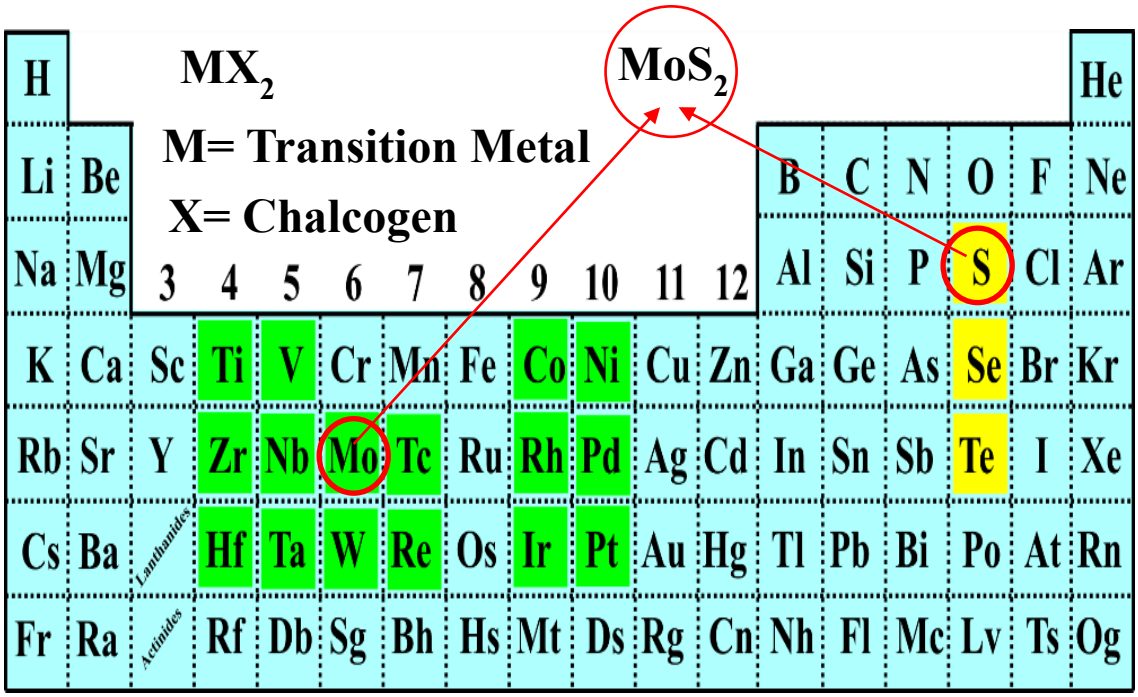

Figure 1.1 *Schematic diagram of periodic table with highlighted transition metals (green in colour) and three chalcogen elements (yellow in colour)[21].*

TMDs are the most promising materials among the 2D materials family for next generation technology, and possess unique physical and electronic properties [7, 22]. The general formula for single-layered TMDs is MX_2, where M represents the transition metal and X represents the chalcogen atom. In periodic table, group IV to group X are considered as transition metals (**Figure 1.1**) and have different numbers of d-electrons [8]. Thus, TMDs express a wide array of electronic nature, including metallic, semiconducting and insulating properties. These materials form different 2D layered materials of the form X-M-X, where the metal atom is sandwich between two

chalcogenide atoms. The position of M and X atoms in the TMDs structure determine whether it is semiconducting or metallic. The layered TMDs such as MoS_2, WS_2, $MoSe_2$, and WSe_2, have been identified as semiconducting 2D layered materials [23, 24]. In the following section we will discuss in details the structure and physical properties of MoS_2.

1.2.1 Structure of MoS_2

A single layer MoS_2 consists of S-Mo-S, where Mo atom is sandwiched between S atoms. The schematic diagram of mono and bi-layer (side view) MoS_2 is shown in **Figure 1.2 (a)**. It has been experimentally observed that thickness of each layer is around 6.5 to 7 Å in layered MoS_2 structure [25, 26]. The top view of MoS_2 is shown in **Figure 1.2 (b)** and the black marked region is the unit cell of MoS_2**.** In case of 2D TMDs material like MoS_2, the adjacent layers are weakly held together to form the bulk crystal in a different polytypes, which are discussed in following section. In this structure, intra-layer Mo-S bonds are covalent in nature, but the layers are coupled by van der Waal forces. The van der Waal force is several orders of magnitude weaker than the in-plane covalent bonding. It has been observed that the metal atoms give four electrons to fill the bonding states of MoS_2, where the oxidation states of the metal (Mo) and chalcogen (S) atoms are +4 and –2, respectively [8].

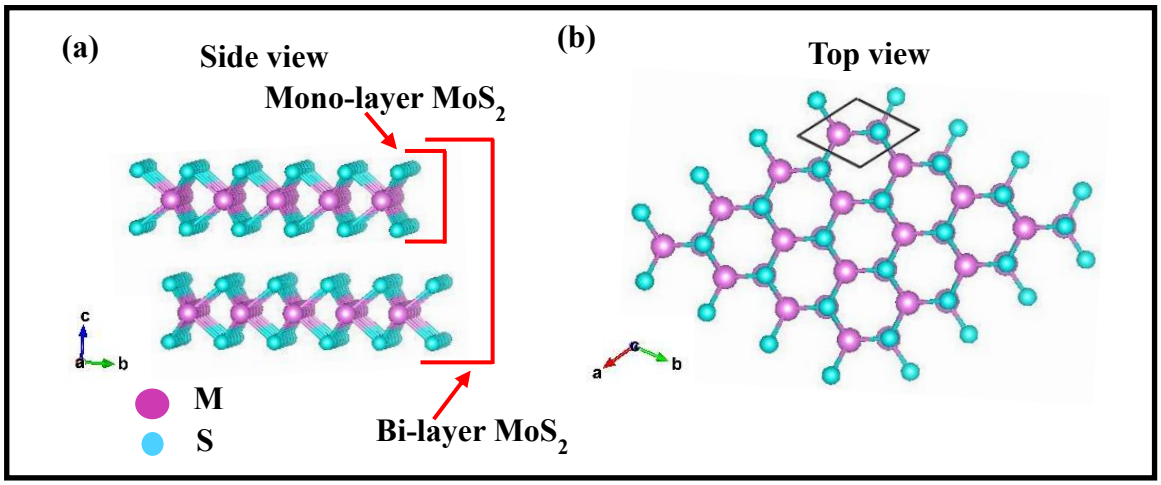

Figure 1.2 *Schematic diagram of (a) Side view of MoS_2 and (b) Top view of MoS_2.*

1.2.2 Different Phase of MoS_2

Depending upon the atomic arrangement of Mo and S atom, MoS_2 exists in three distinct phases. The three most commonly observed polymorphs of MoS_2 are 1T, 2H, and 3R, as shown in **Figure 1.3**. The number (1, 2 and 3) represents the layer number in the unit cell, and the letter stands for symmetry (T-trigonal, H-hexagonal, and R-Rhombohedral) [11, 27]. In 2H and 3R phase Mo atom is prismatically coordinated to six surrounding S atoms (trigonal prismatic). However, in 1T phase the Mo atom is anti-prismatically coordinated to six surrounding S atoms (trigonal anti-prismatic/octahedral). Among these three polymorphs of MoS_2, 2H is the most stable and abundant polytype in earth's crust [28, 29]. The structural difference between 2H- and 3R-MoS_2 is observed due to different arrangement of layers. Both 2H and 3R phases of MoS_2 show similar properties like semiconducting and diamagnetic behaviour, however exhibit different band structure [28]. In contrast, 1T- MoS_2 shows paramagnetic and metallic behaviour.

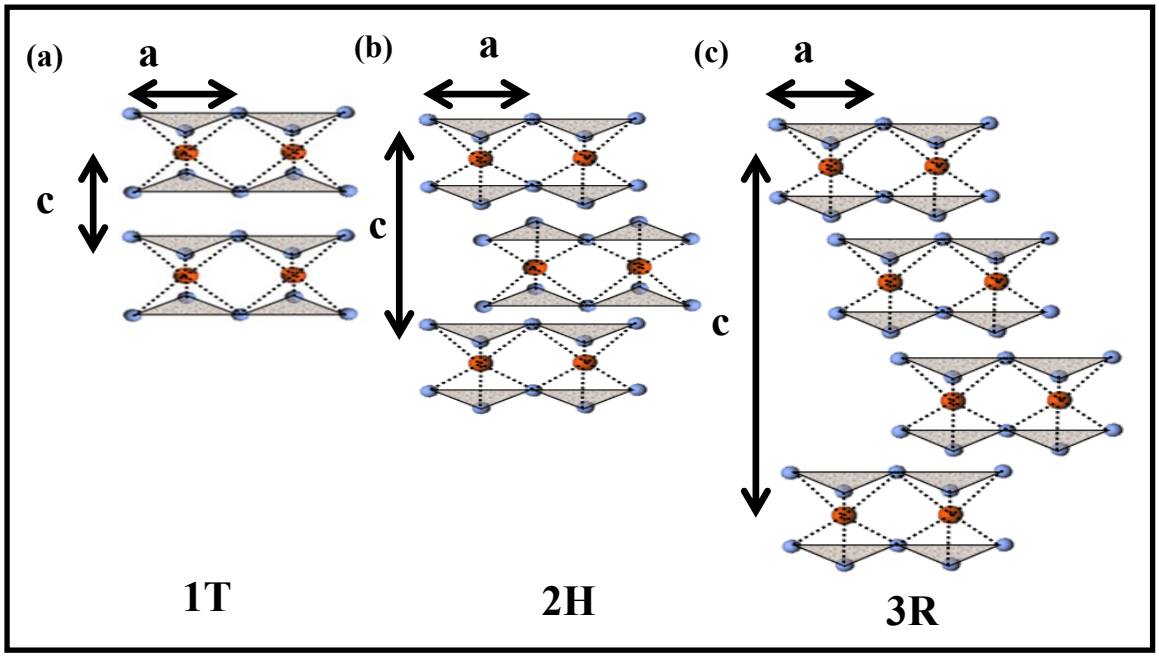

Figure 1.3 *Schematic diagram of MoS_2 polytypes (a) 1T phase (tetragonal symmetry, one layer per repeat unit, octahedral coordination) (b) 2H phase (hexagonal symmetry, two layers per repeat unit, trigonal prismatic coordination) (c) 3R phase (rhombohedral symmetry, three layers per repeat unit, trigonal prismatic coordination) [11].*

1.2.3 Raman Study of MoS_2

Raman spectroscopy is one of the finest non-destructive, quick tools to determine the layer numbers and the phase of 2D materials like MoS_2 [30]. The Bulk MoS_2 and even layer MoS_2 belong to the space group P63/mmc (point group D_{6h}). The primitive unit cell consists of two Mo atoms and four S atoms in sites with point groups D_{3h} and C_{3v}, respectively, which result in 18 Brillouin zone center (Γ) phonons [31]. The irreducible representation of the phonon modes for such a system is $\Gamma = A_{1g} + 2A_{2u} + B_{1u} + 2B_{2g} + E_{1g} + 2E_{1u} + E_{2u} + 2E_{2g}$, where three modes ($2A_{2u} + E_{1u}$) are acoustic and fifteen modes ($A_{1g} + A_{2u} + B_{1u} + 2B_{2g} + E_{1g} + E_{1u} + E_{2u} + 2E_{2g}$) are optical. Among them, the Raman active modes are $2E_{2g}$, E_{1g}, and A_{1g} and the infrared active modes are A_{2u} and E_{1u}. The 2-fold degenerate E symmetry and A modes represent in-plane (shear) vibrations and the out-of-plane vibration (breathing), respectively [32]. The Raman active modes in MoS_2 are shown schematically in **Figure 1.4**.

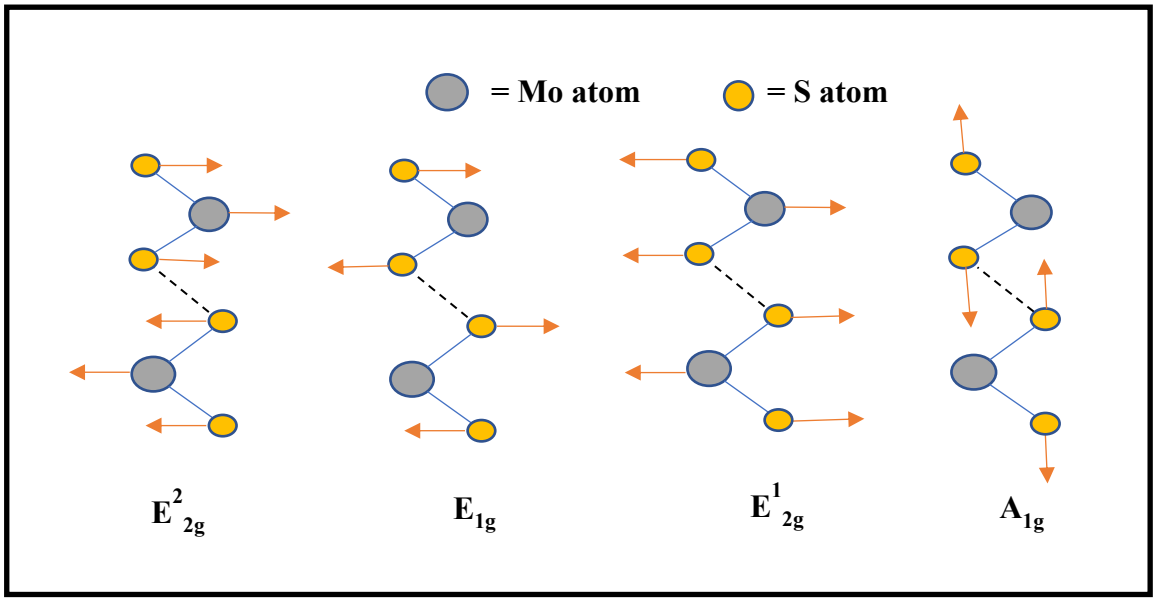

Figure 1.4 *Schematic representation of different Raman active modes of MoS_2 [31].*

Raman spectroscopy can be used to distinguish the phases like 2H and 1T. The characteristic three peaks of octahedral 1T phase appears around 156, 226 and 323 cm^{-1}. These additional three peaks are not observed in the Raman spectrum of 2H-MoS_2 [33, 34]. In case of 2H bulk MoS_2, the E^1_{2g} and A_{1g} peak appears around ~382 cm^{-1} and 408 cm^{-1}, respectively. In general, E^1_{2g} and A_{1g} modes are easily accessible, while E^2_{2g} mode is observed at very low frequencies (~32 cm^{-1}). The E_{1g} mode is forbidden in backscattering geometry on a basal plane. In case of MoS_2, separation between E^1_{2g} and the A_{1g} modes determines the number of layers present in MoS_2 nanostructure [35].

1.3 Synthesis of MoS_2 Nanostructures

In order to use the two-dimensional (2D) MoS_2 nanostructure in technological applications such as photodetectors, phototransistor, display devices etc., growth of superior quality and large area 2D-MoS_2 nanostructures are needed. There are two general methods to synthesize nanostructures like 2D-MoS_2: top-down and bottom-up approach. The top-down approach includes three different synthesis methods, which are mechanical exfoliation, liquid phase exfoliation and Lithium-ion intercalation methods [36-38]. These exfoliation processes are suitable for synthesis of 2D materials due to the weak van der Waal force between the layers, that allows individual 2D layers to be separated from their bulk counterpart. On the other hand, bottom-up approach includes the physical vapor deposition (PVD), chemical vapor deposition (CVD) and solution chemical (hydrothermal/solvothermal) process. In the following section we have discussed these processes separately.

1.3.1 Top-down Approach for MoS_2 Synthesis

In this approach, 2D MoS_2 nanostructures are synthesized from its bulk counterpart. Different top-down approaches are discussed below.

1.3.1.1 Mechanical Exfoliation

It is based on the peeling process of layered materials by application of mechanical force for the synthesis of one or few monolayers. The scotch assisted mechanical peeling is still a widespread approach for making a top-quality 2D sheets of Graphene and TMDs materials. High quality MoS_2 can be synthesized via this method quickly as the mechanical force can overcome the van der Waal interaction between layers. The quality of the film prepared by this technique is known to be highest. Oriol *et al.* used this exfoliation method to synthesize MoS_2 monolayer and showed its suitability for ultrasensitive photodetection [36]. However, the main demerits of this method are the low yield and the small flake size. Therefore, MoS_2 synthesis via this process is limited to the fundamental study at laboratory level.

1.3.1.2 Liquid Exfoliation

Liquid exfoliation method is an important and widely used top-down approach for synthesis of layered nanostructures. In this method, the common organic solvents and/or functionalization are used to exfoliate the bulk materials by various mechanical processes like sonication, shearing, stirring, grinding and bubbling methods. The direct sonication process depends on the solvent and/or surfactant to defeat the cohesion between adjacent layers. Thus, the solvent must be chosen to have surface tension close to the surface energy of the material [39]. This method yields random materials shape, size and layer numbers. Mishra *et al.* synthesized few layer MoS_2 and WS_2 via sonication of their bulk powders using soapy water as solvent [38]. The yield of liquid exfoliation was drastically improved in comparison to mechanical exfoliation technique, however defects are also observed in flakes. This method is suitable where nanomaterials are needed in large amount and defects do not vastly affect applications such as energy

production and storage applications. This process is a cost effective and simple technology for large scale production of 2D MoS_2 nanosheets.

1.3.1.3 Lithium Ion Intercalation

In this method, the small radii ions are intercalated into the adjacent layers in bulk layered materials. Generally, Lithium ion is used to intercalate between layers of 2D materials to expand the interlayer spacing. Generally, N-butyl lithium is used for Li intercalation between layers of TMD material [26]. The single layer MoS_2 was demonstrated by Joensen and co-workers using n-butyl lithium dissolved in hexane [40]. The main problem with this method is that, during the synthesis/intercalation process the Li atoms intercalate in the layer of MoS_2 and the semiconducting 2H phase of MoS_2 transforms into its metallic 1T phase. This method is likely to be better suited for applications in energy storage and generation, sensing or as filler materials for composites where large quantity of materials is required.

1.3.2 Bottom-up Approach for MoS_2 Synthesis

In this approach, 2D materials are synthesized from atoms to cluster formation and finally the nanostructure. Different bottom-up techniques are discussed in the following section.

1.3.2.1 Physical Vapor Deposition (PVD)

In PVD process, material turns into vapour and then condensed onto a surface of a specimen. This technique is used to produce thin film or coating. The coating on the surface of the materials improves the hardness, durability, chemical and oxidation resistance of materials. The most common PVD processes are thermal evaporation, sputtering and arc vapour deposition.[41] In thermal evaporation technique, the coating

materials (source) are heated via hot filament or electrical resistance heating to form vapor. Plasma is generated electrically in between the coating species and substrate in sputtering process. In arc deposition technique, a high-power electric arc is used to vaporize cathode materials, which condenses on a substrate to form a thin film. Muratore *et. al.* showed the synthesis of ultra-thin MoS_2 films at low-temperature by magnetron sputtering [42].

1.3.2.2 Chemical Vapor Deposition (CVD)

CVD technique is known as one of the best techniques to synthesize high quality and large area monolayer of 2D materials. In this process, chemical reaction occurs among different precursors in vapour state and solid-state thin film is deposited as a desired product. In the present work, we have synthesized different MoS_2 nanostructures using CVD technique and details of this technique has been given in **chapter 2**.

1.3.2.3 Solution Chemical Process

There are two different methods for synthesis of 2D materials by this process, hydrothermal and solvothermal processes [43, 44]. In synthesis process of MoS_2 nanostructures, molybdate reacts with sulfide compounds or sulfur in autoclave in temperature range 150-240 °C for several hours. This method yields powder MoS_2 with different shapes and size. The main dissimilarity between these two methods is that the precursor solution in the solvothermal is usually non-aqueous, however in hydrothermal method it is aqueous.

1.4 Properties and Applications of MoS_2 Nanostructures

The physical and chemical properties play important role in application of materials. Some of the physical properties of MoS_2 are discussed in following section.

1.4.1 Electronic Properties

The atomic arrangement of transition metals and their *d*-electron count determine the electronic structure of different TMDs nanostructures like MoS_2 [8]. The electronic properties of 2D MoS_2 depend upon many factors such as thickness, environment, mechanical strain etc. The 2D MoS_2 materials show high carrier mobility and good electrical conductivity compared to conventional semiconductors, making them suitable for developing ultra-broadband photodetectors for use in different areas such as surveillance and sensor for real-life applications. The CVD-grown MoS_2 generally exhibits an n-type semiconducting nature with room temperature carrier mobility in the range of 50-200 $cm^2\ V^{-1}\ s^{-1}$ [13, 45]. The value of the electrical conductivity of MoS_2 is observed in a range of 0.01 to 10 S m^{-1} at room temperature. The value of the electrical conductivity of monolayer MoS_2 can be tuned directly through substitutional doping [46].

1.4.2 Optical Properties

The optical properties of 2D materials depend upon the number of layers. The transparency of 2D material is very crucial for optoelectronic applications. The TMDs materials such as MoS_2 has an indirect optical bandgap in bulk phase with a valence band maximum (VBM) at the Γ point and a conduction band minimum (CBM) at the midpoint along Γ–K symmetry lines. As the thickness is reduced to monolayer, its optical bandgap transforms from an indirect to a direct gap with VBM and CBM coinciding at the K-point. This indirect to direct bandgap transformation occurs due to quantum confinement effect in TMDs [47-49]. The light absorption coefficient (α) of MoS_2 ranges from 5 to 9% per layer in the visible range, which is higher than graphene (2.3 % per layer) [50]. Zhang *et al*. measured the absorption coefficient of mono and bi-layer MoS_2 in suspended and supported cases, and showed absorption coefficients of 5.2 % and 5.8 % for

suspended and supported monolayer MoS_2, respectively. The suspended and supported bi-layer MoS_2 shows absorption of 11.5% and 12.1 %, respectively [51].

1.4.3 Thermal Properties

Thermal properties of materials are crucial in device applications. Thermal expansion coefficient (TEC) of 2D materials provides the information about anharmonic vibrations of low-dimensional system. The in-plane TEC of monolayer MoS_2 is observed around $7.6 \pm 0.9 \times 10^{-6}$ K^{-1}, which is larger than that of bulk MoS_2 ($\sim 4.9 \times 10^{-6}$ K^{-1}) [52]. The TEC of MoS_2 flakes on a glass substrate ranges from 7.5×10^{-6} to 8.5×10^{-6} K^{-1}. Thermal conductivity of 2D materials also depends on the thickness of the materials and substrate and is dominated by phonon transport and ballistic conduction. Thermal conductivity of 2D MoS_2 is moderate as compared to the monolayer graphene and it changes with the layer numbers in MoS_2 nanostructures [53]. Measured room temperature in-plane thermal conductivities of multilayer thin film and bulk MoS_2 are found around 30-35 W m^{-1} K^{-1} and 110 W m^{-1} K^{-1}, respectively [54-56]. Theoretical calculation suggests in-plane thermal conductivities of ~80 and ~ 390 W m^{-1} K^{-1} for multilayer thin film and bulk MoS_2, respectively [57, 58]. The experimentally measured room temperature in-plane thermal conductivity for monolayer and few-layer MoS_2 is found in the range 1.5 to 84 W m^{-1} K^{-1} using optothermal Raman technique [51,53,59]. The defect sites in MoS_2 also reduces its thermal conductivity. The substrate supported film of MoS_2 shows relatively low thermal conductivity as compared to the free standing one because of phonons leaking across the material-substrate interface and interfacial scattering [51].

1.4.4 Applications of 2D MoS_2 Nanomaterials

The 2D-MoS_2 nanostructures have the capability to play a fundamental role in the future of nanoelectronics, optoelectronics, flexible devices, catalysis, sensing, energy generation and storage applications [60-66]. Some of the key area of applications of MoS_2 nanostructures are shown schematically in **Figure 1.5**. The monolayer and few-layer MoS_2 can be used for optoelectronic and photonic applications such as photodetection, optical sensing, solar cells etc. Additionally, MoS_2 nanostructures are found suitable as electrode material in supercapacitors and batteries for energy storage applications. The catalytic activity and effective surface area of MoS_2 can also play a vital role in electrochemical hydrogen production and electrochemical sensing. In the present work, we have used thermal conducting MoS_2 nanostructures for photodetection and Surface enhance Raman spectroscopy (SERS) applications.

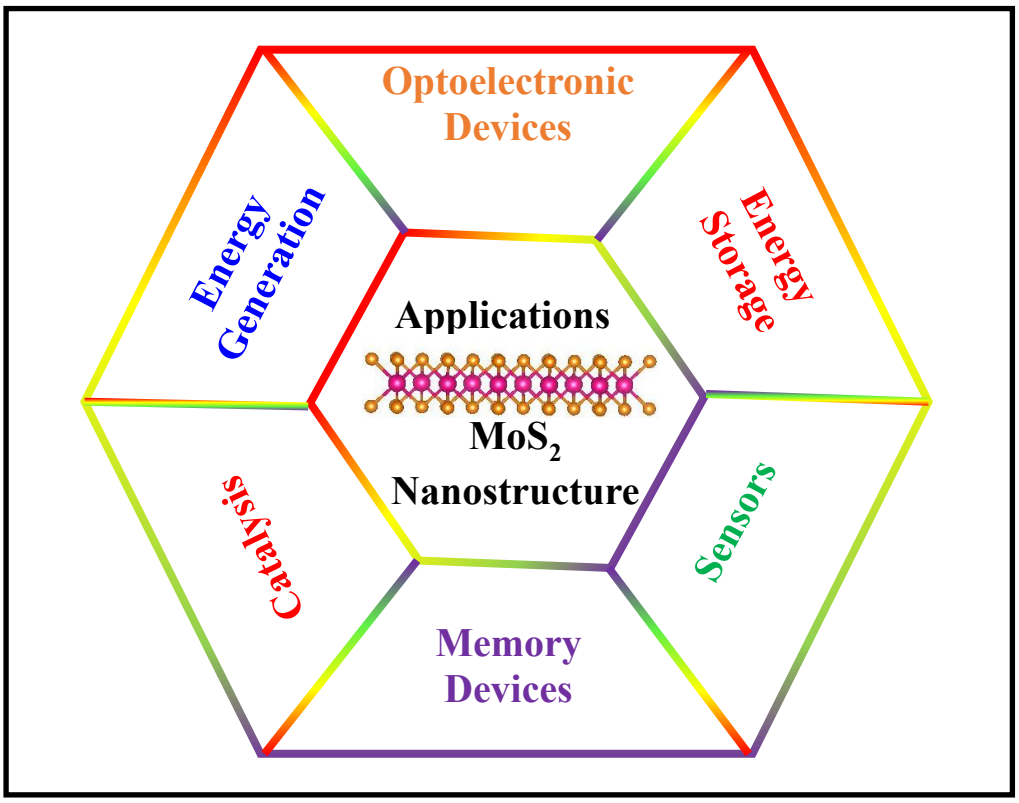

Figure 1.5 *Applications of 2D MoS_2 nanostructures.*

1.5 Thermal Conductivity of 2D MoS_2 Nanostructure

Thermal properties of low dimensional materials are very important in fundamental and application point of view. Thermal management in nanoelectronic and optoelectronic devices is a major issue for their effective performance. There have been limited studies on thermal transport in 2D TMDs due to their challenging fabrication process and suitable thermal measurement methods. Among thermal transport properties, thermal conductivity suggests that how good it conducts heat through the materials. The heat inside the materials is carried by the electrons and acoustic phonons. The total thermal conductivity of a material is the sum of two components and it can be expresses as-

$$K = K_p + K_e \tag{1.1}$$

where K_p and K_e represent phonon and electron contributions to thermal conductivity, respectively. Thermal conductivity of 2D materials is mostly dominated by the phonon contribution [67]. In the following section some of the thermal conductivity measurement techniques have been discussed.

1.5.1 Different Technique to Determine Thermal Conductivity

To measure the thermal conductivity of 2D materials (thin films), multiple experimental and theoretical efforts have been applied [68-70]. Different experimental techniques to determine thermal conductivity of low dimensional systems are briefly discussed as follows-

Optothermal Raman Technique

Traditionally Raman spectroscopy is used as a non-destructive footprint technique for the detection of the vibration modes in the materials. However, a large

amount of information can be extracted by observing the change in peak positions and peak width due to the external stimuli such as pressure and temperatures. Among different methods, optothermal Raman (OTR) technique is mostly used to determine the thermal conductivity of low dimensional materials (1D and 2D) [71]. The schematic diagram of typical configuration of OTR technique is shown in **Figure 1.6**. In this method, 2D material is either suspended over a hole/trench or supported by substrate. In this noncontact technique, Raman spectra act as an effective "thermometer" to measure thermal conductivity of 2D materials. This method was first applied to measure the thermal conductivity of single-layer graphene in 2008 [72]. In this technique, laser light of a desirable wavelength acts as a heat source to generate a local temperature rise in the film, which produces the shifting in the Raman modes. Further, shift in Raman modes is also observed at fixed laser power but at different sample temperatures. Under the assumption that the heat propagates radially, thermal conductivity of 2D materials is calculated using appropriate models.

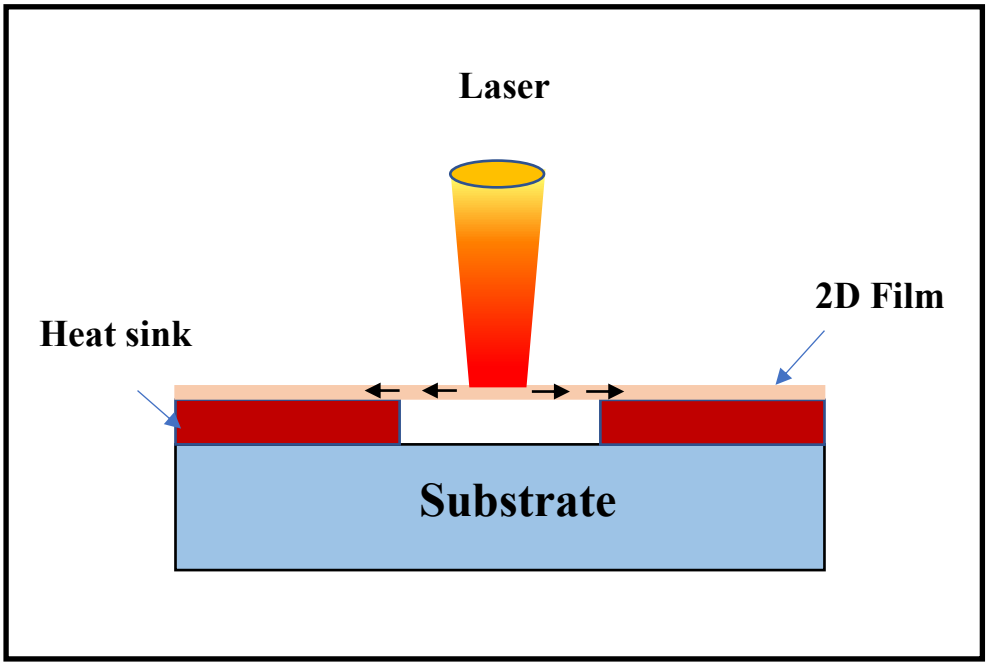

Figure 1.6 *Schematic diagram of optothermal Raman technique. Black arrow shows the direction of heat flow [72].*

Thermal Bridge Method

In 2001, Kim *et al*. used electron beam lithography and a nano-manipulation for thermal bridge method to determine the thermal conductivity of individual multi-walled carbon nanotube [73]. In this method, a microelectromechanical system (MEMS) device and nano-manipulation system are used to detect the change in temperature at micro/nano scale. A metal thin film resistor serves as a heating source to increase the temperature of the suspended sample. The change in resistance of metal resistor with temperature act as thermometer.

3Omega (3ω)-Method

The 3ω-method is a technique to measure thermal conductivity of bulk material and thin films [74]. In this method a thin metal structure is used for resistive heating of sample periodically using alternating current. Temperature response of the sample is measured across a range of frequencies. The linear slope of ΔT vs. $\log(\omega)$ curve is used to determine the thermal conductivity.

Time-Domain Thermo Reflectance (TDTR) Technique

Thermal conductivity of thin films (thickness less than 100 nm) and thermal conductance at interface are precisely measured by TDTR technique [75]. In this technique, when the material is heated up, during that time the reflectance of the surface changes and is measured with respect to time which can be used to determine the thermal properties.

Scanning Thermal Microscope (SThM) Technique

Scanning thermal microscopy (SThM) technique allows the thermal measurement at the nano-scale. In 1986, it was invented by Clayton C. Williams and H. Kumar

Wickramasinghe [76]. This is a type of scanning probe microscopy which provides the information about the temperature mapping and thermal conductivity across a sample surface. In this method, heat flows from a probe to the sample and amount of heat flow changes with scanning, which provides the thermal mapping and spatial variations in thermal conductivity of a sample.

Thermal Flash Method

Thermal conductivity of a materials can be calculated by this method using a fundamental relationship $k= \alpha \rho C_p$, where k, α, ρ, C_p represent thermal conductivity, thermal diffusivity, density and specific heat capacity of the material, respectively. In this technique, prior knowledge of ρ and C_p is essential to determine the thermal conductivity of a material [77]. In this method, temperature rise at the rear face of the thin sample is measured due to short energy pulse on the front face.

1.5.2 Literature Survey on Thermal Conductivity of MoS_2 Nanostructures by OTR Method

Researchers have successfully used optothermal Raman (OTR) technique to measure the thermal conductivity of 2D materials. Yan *et al.* performed OTR technique to determine the thermal conductivity (~34.5 ± 4 W m^{-1} K^{-1}) of mechanically exfoliated monolayer of MoS_2 over 1.2 μm wide holes of Si_3N_4 grid [78]. Sahoo *et al.* calculated thermal conductivity of few-layer suspended MoS_2 film to be ~52 W m^{-1} K^{-1} at room temperature [79]. Bae *et al.* showed thermal conductivity of 43.4 ± 9.1 W m^{-1} K^{-1} for suspended multilayer MoS_2 using OTR method [53]. Li *et al.* calculated thermal conductivity of monolayer suspended MoS_2 with value ~ 40.8 ± 0.8 W m^{-1} K^{-1} at room temperature (300 K) [80]. Jo *et al.* studied the thermal conductivity of suspended exfoliated few-layer MoS_2 samples and found the room-temperature thermal

conductivities to be (44–50) and (48–52) W m^{-1} K^{-1} for four- and seven-layers thick samples, respectively [81]. Yu *et al.* calculated the thermal conductivity of multi-walled MoS_2 nanotube in the range of 4.8 ± 0.1 to 11.1±0.2 W m^{-1} K^{-1} [82]. Gertych *et al.* found very low thermal conductivity around 1.5 W m^{-1} K^{-1} at room temperature for multilayer MoS_2 thin film (65 nm) by statistical OTR technique [59]. Judek *et al.* calculated the thermal conductivity of 67±5 W m^{-1} K^{-1} for supported multilayer MoS_2 film over SiO_2/Si substrate [83], while Yu *et al.* obtained the thermal conductivity of ~32.5±3.4 W m^{-1} K^{-1} for CVD grown monolayer MoS_2 over 1.8 μm wide holes [84]. Liu *et al*. investigated thermal conductivity of MoS_2/InSe-NPs/MoS_2 and MoS_2/MoS_2 samples on SiO_2/Si substrate with values of ~102.3 W m^{-1} K^{-1} and ~81.7 W m^{-1} K^{-1}, respectively [85]. In the present work, we have also used OTR technique to measure the thermal conductivity of CVD grown MoS_2 nanostructured films.

1.6 Photodetection Applications of MoS_2 Nanostructure

The detectors are the devices that detects the existence of a specific type of signal and convert it to some other form of signal that can be understood easily. Photodetectors are optoelectronic devices called the photosensors, which sense/detect the electromagnetic radiations by converting photons (light) into electric charges [86]. Photodetectors are becoming a key component of optoelectronic technology because of their wide range of applications. Its basic principle is based on the light absorption and generation of photocurrent or photovoltage within the device. The photodetector device can be in different form like photoconductor, photodiode and phototransistor. The efficiency of a photodetector depends on many factors such as the optical absorption coefficient, charge carrier generation and transport. A large number of semiconducting materials are used as active materials, but each material has some advantages and

disadvantages in view of fabrication process, stability and efficiency. The group of semiconducting TMDs are emerged as a promising candidate for optoelectronic devices in view of their ultimate scalability down to the atomic level and presence of suitable bandgap. Few-layer MoS_2 based photodetectors show relatively higher photoresponsivity as compared to graphene-based photodetectors due to the presence of finite direct band gap and strong light absorption [87-90]. The electromagnetic spectrum covered by 2D MoS_2 is marked in the schematic diagram of **Figure 1.7**. The semiconducting 2H-MoS_2 is found stable material with bandgap in the visible range suitable for visible range photodetectors [91].

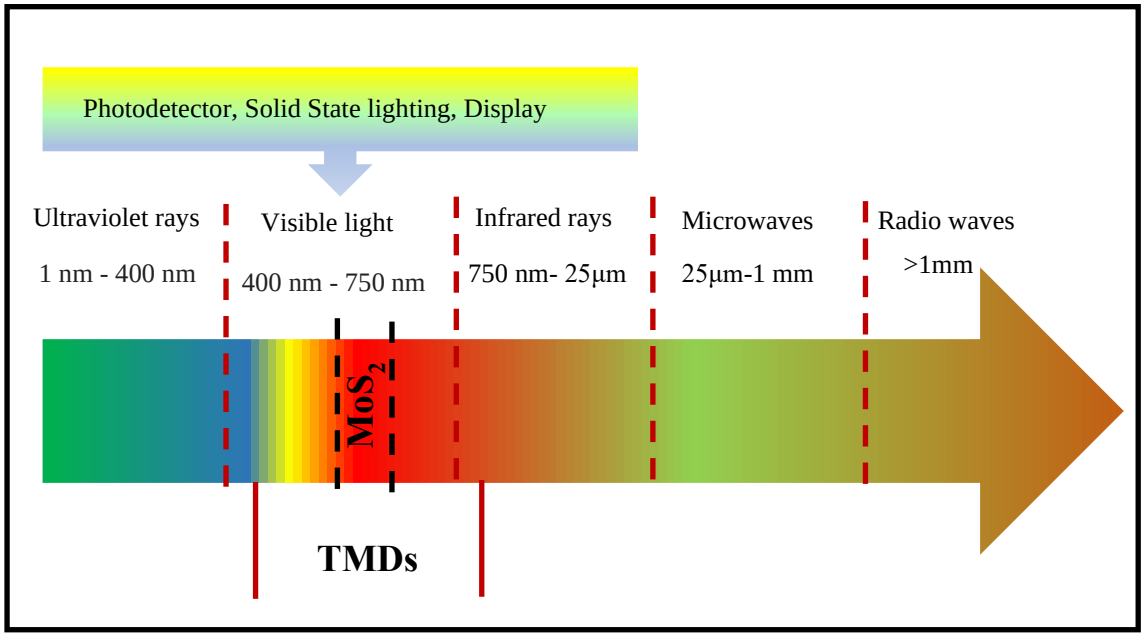

Figure 1.7 *The electromagnetic spectrum of 2D TMDs [91].*

1.6.1 Basic Principle of Photodetection Process

Photodetectors are based on the quantum photoelectric effect in which the incident light interact with the material and causes a change in conductance or produce a photocurrent or photovoltage. In this section, we will discuss the primary mechanisms

involved in photodetectors. The two main mechanisms are photoconductive and photovoltaic effects used for the photodetection purpose, which are briefed as follows-

Photoconductive Effect

In this process, electron-holes are generated in the semiconductor system when the energy of the incident light (photon) is higher than the band gap of a materials. It induces the change of carrier density and increases the electrical conductivity as follows-

$$\Delta\sigma = \Delta nq\mu \tag{1.3}$$

where σ, n, q and μ represent the electrical conductivity, charge carrier density, elementary charge and the mobility of the photoactive material. The band diagram of p-n junction under photoconductive mode is shown in **Figure 1.8**.

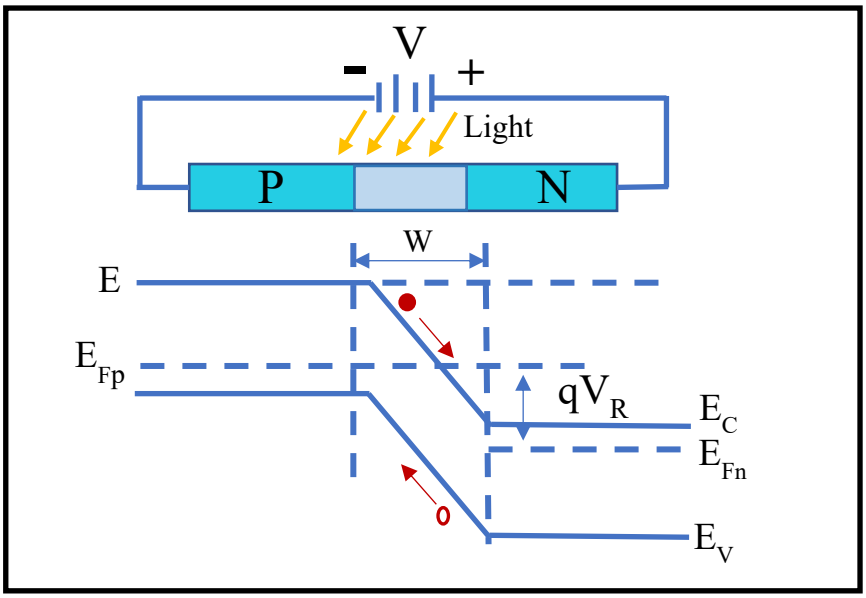

Figure 1.8 *Band alignment of p-n junction under photoconductive mode [92].*

In this effect, photogenerated charge carriers (electron–hole pairs) drift in opposite directions by built-in electric field and the external applied field. It greatly reduces the possibility of recombination of generated charge carriers. Under the reverse bias condition across the junction, the internal electric field will be increased and the energy

barrier increases by qV_R as shown in **Figure 1.8**. Under reverse bias condition the photogenerated electron and holes are drifted more easily, i.e the electrons and holes are separated more effectively [92].

Photovoltaic Effect

In this effect, photogenerated charge carriers are decoupled by intrinsic built-in electric field rather than the applied bias voltage. The open circuit voltage can be developed by the accumulation of the carriers of opposite polarities, which leads to the separation of charge carriers resulting in large photocurrent [92]. The built-in electric field at junction effectively separate the charge carrier and produces a reasonable short-current Isc at V=0. The band alignment of p-n junction under photovoltaic mode is shown in **Figure 1.9**.

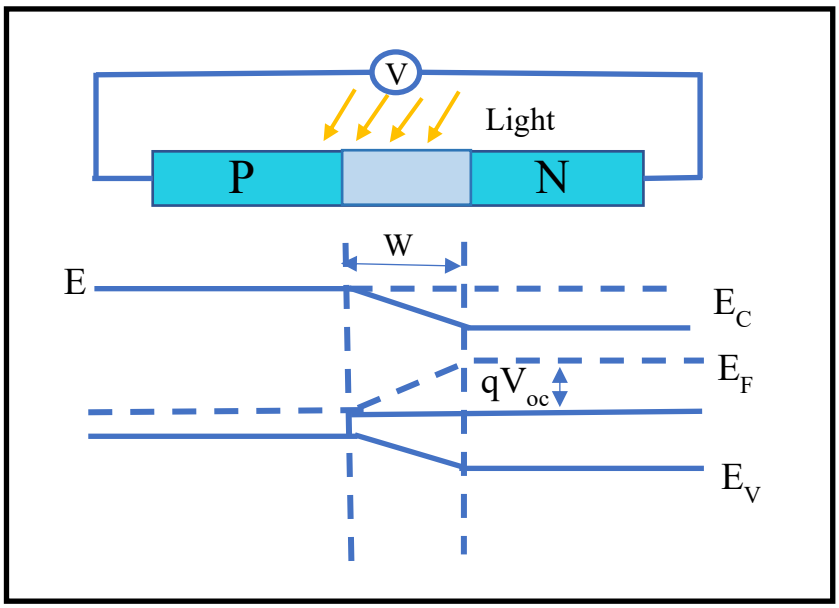

Figure 1.9 *Band alignment of p-n junction under photovoltaic mode [92].*

1.6.2 Literature Survey on Photodetection Application of MoS_2 Nanostructure

Among the TMDs family, MoS_2 has been established as an intriguing building block for the next generation optoelectronics, such as photodetectors due to the presence

of direct bandgap of around 1.8 eV in monolayer form with high mobility. Most of the TMDs show emission in visible and near-infrared region of the spectrum [93]. The presence of direct electronic transitions in monolayer MoS_2 increases the probability for excitons (electron-hole pairs) generation [92, 94]. The MoS_2 (monolayer and few-layer) show emission in the red region of the visible light, as shown in **Figure 1.7**. Different research groups have investigated MoS_2 based photodetector in the visible range and are trying to improve the performance. Mukherjee *et. al.* demonstrated MoS_2 quantum dot/Si photodetector for the detection of visible light (514 nm) and found the photoresponsivity of ~ 2.8 A W^{-1} at -2 V [95]. Qiao *et al.* reported the synthesis of few-layer V-type MoS_2 over Si substrate via CVD technique and observed the photoresponsivity of the heterojunction device around ~0.908 A W^{-1} under the 808 nm laser illumination [96]. Mukherjee *et al*. observed the responsivity 0.47 A W^{-1} of the hybrid 2D/3D MoS_2/Si heterostructures with superior junction characteristics under the illumination of 514 nm laser [97]. Liu *et al.* synthesized monolayer MoS_2 via CVD technique and transferred it over p-type Si substrate to make heterojunction photodetector. They observed photoresponsivity ~ 117 A W^{-1} at 3V reverse bias for the device under incident light intensity of 0.95 mW [98]. Zhang *et al.* reported 2D MoS_2/GaN heterostructure for photodetection application with photoresponsivities of ~328 A W^{-1} and ~27.1 A W^{-1} under visible and UV light illumination, respectively [99].Ye *et al.* fabricated near-infrared photodetector based on MoS_2/black phosphorus heterojunction with photoresponsivity of ~ 22.3 A W^{-1} and ~0.1534 A W^{-1} for the wavelengths 532 nm and 1.55 μm, respectively [100]. Guo *et al.* fabricated broadband photodetector based on vertically stage-liked MoS_2/Si heterostructure having photoresponsivity of 0.746 A W^{-1} at applied voltage -2 V under 808 nm light illumination [101] Lu *et al.* studied the photoresponse behaviour of multilayer/monolayer MoS_2 junction with photoresponsivity

of the device around 0.12 AW^{-1} under 532 nm laser excitation at applied voltage 3 V [102]. Tsai *et. al.* reported few-layered MoS_2 based photodetector with high broadband photogain for use in harsh environments. They found the photoresponsivity~ 0.57 A W^{-1} under the excitation of 532 nm laser [103].

1.7 Surface Enhanced Raman Spectroscopy

Among various sensing technologies, optical methods shows potential in quick detection of analyte molecules [104]. Raman spectroscopy is used for compound fingerprinting, like other optical sensing methods such as Fourier transform infrared, UV-visible absorption and fluorescence spectroscopy. However, Raman technique suffers with weak signals due to the small scattering cross-section. Surface enhanced Raman spectroscopy (SERS) is known as an advanced Raman technique suitable for detection of molecules at ultra-low concentrations. SERS technique enhances the Raman signal by improving the interaction between probe molecule and substrate with plasmon resonance or charge transfer [105, 106]. As a first demonstration, Fleishmann and his group showed the Raman signal enhancement for pyridine molecule over roughened silver surface in 1974 [106]. The metal (Ag, Au, Cu) SERS substrates are widely used with Raman signals amplification of 10^6-10^{14} times for the molecules, while semiconductor SERS substrates exhibit moderate amplification (10^3 times) [107]. The lower cost value, higher chemical stability, suitable band gap and refractive index of semiconductors can help to develop cost effective SERS technology [108-110]. The tunable bandgap, appropriate surface roughness and active sites of different morphologies of MoS_2 nanostructures can improve the effective light trapping and dye adsorption for efficient detection of analytes [111, 112].

1.7.1 Theories for SERS Enhancement

In order to understand the reason behind the enhanced signal in SERS process, mainly two different theories (electromagnetic and chemical mechanism) are known. Gersten discussed in 1980 that the surface plasmons play a key role in SERS signal enhancement on metal substrates [113-115]. The collective oscillations of the conduction electrons in metals i.e. surface plasmons are responsible for SERS electromagnetic (EM) enhancement. The oscillations of conduction electrons in metal nanoparticles due to the oscillating incoming excitation cause a generation of Hertzian dipole on the nanoscale, which can emit frequency as same as of incident wave. The enhanced localized electric field around the metal nanostructure induces another dipole moment in the analyte molecule. The plasmon resonance lies in the visible or near UV region for metals (like Ag and Au) [116]. Chemical enhancement depends on the local electronic structures of analyte and the SERS substrate [117, 118]. It is the combination of non-resonant charge in the molecular polarization, charge transfer between analyte and substrate and enhancements from molecular excitation resonances. The enhancement effects are multiplicative when both the mechanisms are simultaneously working in SERS process. The Herzberg–Teller coupling explains the reason behind SERS signal enhancement, which includes the surface plasmon resonance (SPR), charge-transfer resonance and molecular resonance [112, 116]. **Figure 1.10** depicts a hypothetical illustration of the spectral and relative magnitude distribution of different enhancement mechanisms. It shows relatively higher magnitude of electromagnetic enhancement among other enhancement mechanisms. Non-resonant chemical enhancement is independent of excitation frequency and provides moderate enhancement between 10^0 and 10^2 [119]. The excitation wavelength (resonance condition) also plays an important role to enhance the signal [116].

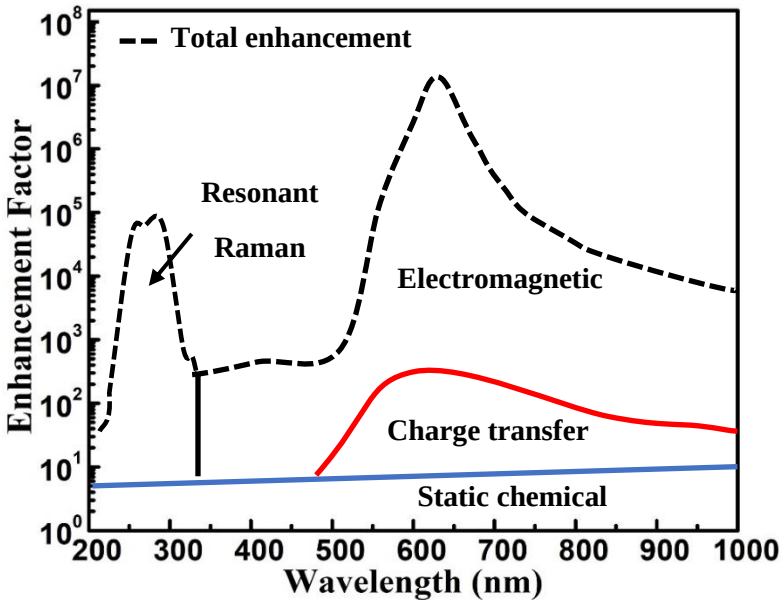

Figure 1.10 *Hypothetical example of the spectral dependence of SERS [119].*

1.7.2 Literature Survey on SERS Application of MoS_2 Nanostructures

In last few years, the scientific community performed SERS study of semiconducting 2D MoS_2 for the detection of organic dyes and biomolecues. Lee *et al*. discussed SERS detection of Rhodamine6G (R6G) molecule using horizontal grown MoS_2 and detected micromolar concentration of R6G [120]. Zheng *et al*. synthesized MoS_2 nanosheets by hydrothermal technique and showed SERS detection of Rhodamine B (RhB) at sub micromolar concentrations (10^{-7} M) [121]. Muehlethaler *et al*. used CVD grown monolayer MoS_2 to detect 4-Mercaptopyridine with enhancement factor around ~ 3×10^5 [66] . Ling *et al.* synthesized MoS_2 nanostructure as SERS substrate to detect the copper phthalocyanine (CuPc) molecule [122]. Er *et al*. prepared 1T MoS_2 by chemical exfoliation and used it as SERS substrate to detect R6G and crystal violet (CV) molecule [123]. Singh *et al.* synthesized 3D-MoS_2 nanoflowers via hydrothermal method with tunable surface area and showed SERS detection of RhB at sub micromolar concentrations 10^{-7} M [124]. Chen *et al.* prepared MoS_2/Ag hybrid substrate for the SERS

detection of 4-mercaptobenzoic acid at sub nanomolar concentrations (10^{-10} M) [125]. Zheng *et al*. hydrothermally prepared MoS_2 nanosheets and used it as SERS substrate to detect RhB molecule at lowest concentration of 0.1 ppm [121]. Sun *et al.* prepared monolayer MoS_2 and used it for pressure induced SERS substrate for the detection of three different dye molecules- methylene blue (MB), phthalocyanine copper (CuPc), and crystal violet (CV) at 10^{-8} M concentration [126]. Rani *et al.* prepared artificial edge in CVD grown monolayer MoS_2 by low-power focussed laser-cutting and drop-casted Au nanoparticles along the artificial edges. They used this MoS_2/Au substrate for SERS detection of RhB molecule at low concentration of 10^{-10} M [127].

1.8 Scope and Objective of the Present Work

The 2D MoS_2 possess some attractive properties such as direct bandgap, layered structure, high-surface area, flexibility, layer-dependent optical bandgap, high absorption coefficient and good stability in acidic/basic environment. Based on these properties, MoS_2 can be utilized in different applications such as photodetector, SERS, energy generation and storage etc. Thermal behaviour of 2D MoS_2 plays a vital role in its utilization in different applications such as heat dissipation in electronic circuit and energy conversion in thermoelectric. Hence, understanding the thermal transport behaviour of 2D MoS_2 is important for its application in electronic and optoelectronic devices. The 2D MoS_2 possesses tunable direct bandgap in the visible range depending upon the number of layers and external environments such as temperature and pressure. Hence it can be utilized for sensing applications such as photodetection and SERS. The main objectives of the present work are as follows-

- To successfully demonstrate the synthesis of different morphologies for 2D MoS_2 nanostructures over Si and SiO_2/Si substrates via CVD technique.

- Investigation of thermal transport behaviour of prepared MoS_2 nanostructures.
- Investigation of thermal sensitive quantum confinement phenomenon in prepared MoS_2 nanostructures.
- Understanding photoresponse behaviour of prepared MoS_2/Si heterojunction.
- Investigating application of prepared MoS_2 nanostructures as SERS substrates for the detection of organic dyes.